Pupil filters for generation of light sheets

Colin J. R. Sheppard

Italian Institute of Technology, Via Morego 30, Genova 16163, Italy
Singapore-MIT Alliance for Research and Technology (SMART) Centre, 1 Create Way, Singapore 138602, Singapore
**colinjrsheppard@gmail.com*

Abstract: Pupil filters for cylindrical (two-dimensional) focusing with extended depth of field are investigated. An important application is in generating light sheets with uniform intensity. Filters for spherical (three-dimensional) focusing with a flat axial intensity, coupled with weak side lobes are also discussed.

OCIS Codes: (050.1220) Apertures; (050.1940) Diffraction; (070.2580) Paraxial wave optics; (110.6980) Transforms; (350.6980) Transforms.

References and links

1. A. H. Voie, D. H. Burns, and F. A. Spelman, "Orthogonal-plane fluorescence optical sectioning: three-dimensional imaging of macroscopic biological specimens," J. Microsc. **170**(3), 229–236 (1993).
2. E. Fuchs, J. S. Jaffe, R. A. Long, and F. Azam, "Thin laser light sheet microscope for microbial oceanography," Opt. Express **10**(2), 145–154 (2002).
3. J. Huisken, J. Swoger, F. Del Bene, J. Wittbrodt, and E. H. K. Stelzer, "Optical sectioning deep inside live embryos by selective plane illumination microscopy," Science **305**(5686), 1007–1009 (2004).
4. H.-U. Dodt, U. Leischner, A. Schierloh, N. Jährling, C. P. Mauch, K. Deininger, J. M. Deussing, M. Eder, W. Zieglgänsberger, and K. Becker, "Ultramicroscopy: three-dimensional visualization of neuronal networks in the whole mouse brain," Nat. Methods **4**(4), 331–336 (2007).
5. C. J. R. Sheppard and X. Mao, "Confocal microscopes with slit apertures," J. Mod. Opt. **35**(7), 1169–1185 (1988).
6. R. Wolleschensky, B. Zimmermann, and M. Kempe, "High-speed confocal fluorescence imaging with a novel line scanning microscope," J. Biomed. Opt. **11**(6), 064011 (2006).
7. E. R. Dowski, Jr. and W. T. Cathey, "Extended depth of field through wave-front coding," Appl. Opt. **34**(11), 1859–1866 (1995).
8. C. J. R. Sheppard and Z. S. Hegedus, "Axial behaviour of pupil plane filters," J. Opt. Soc. Am. A **5**(5), 643–647 (1988).
9. C. J. R. Sheppard, "Binary phase filters with a maximally-flat response," Opt. Lett. **36**(8), 1386–1388 (2011).
10. C. J. R. Sheppard and S. Mehta, "Three-level filter for increased depth of focus and Bessel beam generation," Opt. Express **20**(25), 27212–27221 (2012).
11. C. J. R. Sheppard and T. Wilson, "Gaussian-beam theory of lenses with annular aperture," IEE J. Microwaves, Opt. Acoust. **2**(4), 105–112 (1978).
12. J. Durnin, J. J. Miceli, Jr., and J. H. Eberly, "Diffraction-free beams," Phys. Rev. Lett. **58**(15), 1499–1501 (1987).
13. F. Gori, G. Guattari, and C. Padovani, "Bessel-Gauss beams," Opt. Commun. **64**(6), 491–495 (1987).
14. L. W. Casperson, D. G. Hall, and A. A. Tovar, "Sinusoidal-Gaussian beams in complex optical systems," J. Opt. Soc. Am. A **14**(12), 3341–3348 (1997).
15. C. J. R. Sheppard, "Cylindrical lenses; focusing & imaging: a review [invited]," Appl. Opt. **52**, 1–8 (2013).
16. M. Born and E. Wolf, *Principles of Optics,* 6th ed. (Pergamon, 1993).
17. Y. Li and E. Wolf, "Three-dimensional intensity distribution near the focus in systems of different Fresnel numbers," J. Opt. Soc. Am. A **1**(8), 801–808 (1984).
18. Y. Li, "Three-dimensional intensity distribution in low Fresnel number focusing systems," J. Opt. Soc. Am. A **4**(8), 1349–1353 (1987).
19. C. J. R. Sheppard and K. G. Larkin, "Focal shift, optical transfer function, and phase-space representations," J. Opt. Soc. Am. A **17**(4), 772–779 (2000).
20. C. J. R. Sheppard and H. J. Matthews, "Imaging in high aperture optical systems," J. Opt. Soc. Am. A **4**(8), 1354–1360 (1987).
21. D. M. de Juana, J. E. Oti, V. F. Canales, and M. P. Cagigal, "Design of superresolving continuous phase filters," Opt. Lett. **28**(8), 607–609 (2003).
22. M. P. Cagigal, J. E. Oti, V. F. Canales, and P. J. Valle, "Analytical design of superresolving phase filters," Opt. Commun. **241**(4-6), 249–253 (2004).
23. C. J. R. Sheppard, S. Ledesma, J. Campos, and J. C. Escalera, "Improved expressions for performance parameters for complex filters," Opt. Lett. **32**, 1713–1715 (2007).

#180903 - $15.00 USD Received 29 Nov 2012; revised 11 Jan 2013; accepted 11 Jan 2013; published 6 Mar 2013

1. Introduction

In numerous applications we require to optimize depth of field for a given aperture size, i.e. while maintaining transverse spatial resolution and light collection efficiency. We investigate the use of pupil filters to increase the focal depth for cylindrical focusing systems. We note that there are many practical examples of such two-dimensional (2D) optical systems, including integrated optics (planar waveguides) and plasmonics, and also optical systems such as light sheet microscopy [1–4], line illumination microscopy [5, 6], and cubic phase mask systems [7].

We start by deriving performance parameters for focusing by centro-symmetric cylindrical focusing systems, in analogy with those presented previously for rotationally symmetric spherical focusing systems [8]. We then continue with development of binary phase pupil filters (i.e. those having regions of amplitude $+1$ and -1) that give maximally-flat (MF) axial intensity, using an analytic approach (i.e. not iterative) previously investigated for rotationally symmetric pupils [9, 10].

For the rotationally symmetric case, the solution that gives a completely flat axial intensity is the Bessel beam [11, 12], which is a propagationally-invariant solution of the wave equation. One family of MF solutions derived for the rotationally-symmetric case tends towards a Bessel beam for large number of elements. The Bessel beam contains infinite energy, so approximations such as the Bessel-Gauss beam [11, 13] have been developed, that are finite energy beams exhibiting a more uniform axial intensity than a Gaussian beam. But these approximations to the Bessel beam do not usually give nearly as good axial uniformity as the MF solutions, nor are they band limited, i.e. they do not correspond to a pupil of compact support. The 2D analog of the Bessel beam is the cosine beam, but perhaps this should not be regarded as a beam, because each lobe has the same maximum intensity. The cosine-Gauss beam [14] is the 2D analog of the Bessel-Gauss beam. The cross-section of the beam is the product of a cosine and a Gaussian, while the pupil (far-field) is the product of a hyperbolic cosine and a Gaussian. In the terminology of Ref [11], the amplitude of the cosine-Gauss beam for any point in space can be written very simply as

$$U(v,u) = \frac{e^{ikz}}{\sqrt{1+iub^2}} \cos\left(\frac{v}{1+iub^2}\right) \exp\left[-\frac{(v^2b^2+iu)}{2(1+iub^2)}\right], \tag{1}$$

where b is a dimensionless parameter, v and u are transverse and axial optical coordinates, respectively (given in Eqs. (3), 4 below), and the waist w_0 of the underlying Gaussian is related to the nominal numerical aperture $\sin\alpha$ by $kw_0 b \sin\alpha = \sqrt{2}$, with $k = 2\pi/\lambda$. The axial intensity can be seen from Eq. (1) to stretch out as b becomes smaller, but still the variation near the focus is parabolic.

2. Performance parameters for symmetric, cylindrical focusing systems

We can introduce performance parameters to describe various features of the focusing system for the 2D case, in a similar way to those used for 3D systems [8]. These parameters are useful because they allow the filter performance to be investigated without the necessity for calculating the focused field. These parameters can be used as a design tool, including use as merit functions for iterative optimization. The amplitude in the focal region for a cylindrical lens with pupil function (i.e. the amplitude transmission of the lens pupil) given by $P(\xi)$ in the scalar, paraxial, Fresnel regime can be written [15]

$$U(v,u) = \sqrt{N(z)}\, e^{-i\pi/4} e^{ikz} \exp\left[\frac{iv^2}{4\pi N(z)}\right] \int_{-1}^{1} P(\xi) \exp\left(-\frac{iu\xi^2}{2}\right) \exp(iv\xi)\, d\xi, \tag{2}$$

#180903 - $15.00 USD Received 29 Nov 2012; revised 11 Jan 2013; accepted 11 Jan 2013; published 6 Mar 2013

where, for a system of width $2a$ and focal length f , $\xi = x_{\text{pupil}} / a$ and the optical coordinates in the transverse and axial directions are

$$v = \frac{kf\,x}{z}\sin\alpha = \frac{kxa}{z}, \tag{3}$$

$$u = ka^2\left(\frac{1}{f}-\frac{1}{z}\right) = \left(\frac{f}{z}\right)k\,\delta z\,\sin^2\alpha, \tag{4}$$

respectively (to be consistent with Born and Wolf [16], and Li and Wolf [17, 18]), and $N(z) = a^2/\lambda z$ is a depth dependent Fresnel number [19]. Here the pupil is assumed to be in the plane of the lens. The Debye approximation follows by putting $N \to \infty$ and $z = f$, and is equivalent to the pupil being situated in the front focal plane of the system, at $z = -f$. For a high numerical aperture system in the scalar regime, $\sin^2\alpha$ is then more accurately replaced by $4\sin^2(\alpha/2)$ [20]. Expanding as power series to quadratic terms in v, u , for a symmetrical pupil for large Fresnel number, we obtain

$$\begin{aligned} U(v,u) &= \frac{1}{2}\int_{-1}^{1} P(\xi)\left[1-\frac{(v^2+iu)\xi^2}{2}-\frac{u^2\xi^4}{8}+\ldots\right]d\xi \\ &= \frac{I_0}{2}\left[1-\frac{(v^2+iu)}{2}\frac{I_2}{I_0}-\frac{u^2}{8}\frac{I_4}{I_0}+\ldots\right], \end{aligned} \tag{5}$$

where

$$I_n = \int_{-1}^{1} P(\xi)\,\xi^n\,d\xi \tag{6}$$

is the *n*-th order moment of the pupil, and we have normalized to unity at the origin for a uniform, unobstructed pupil. For a real-valued pupil function (which can nevertheless be negative as in the important case of a binary phase mask), the parabolic approximation to the intensity in the focal region can therefore be written

$$I(v,u) = \frac{I_0^2}{4}\left\{1-v^2\left(\frac{I_2}{I_0}\right)^2-\frac{u^2}{4}\left[\frac{I_4}{I_0}-\left(\frac{I_2}{I_0}\right)^2\right]\right\}. \tag{7}$$

For a complex pupil, which can produce an asymmetric axial intensity and a shift of the primary focus, more complicated expressions need to be used [21–23]. For a uniform, unobstructed aperture, $I_0 = 2, I_2 = 2/3, I_4 = 2/5$, so we can introduce the Strehl ratio and the transverse and axial gain parameters:

$$S = I_0^2,\; G_T = 3\frac{I_2}{I_0}, G_A = \frac{45}{4}\left[\frac{I_4}{I_0}-\left(\frac{I_2}{I_0}\right)^2\right], \tag{8}$$

to give for the focal intensity distribution

$$I(v,u) = S\left(1-\frac{G_T v^2}{3}-\frac{G_A u^2}{45}\right). \tag{9}$$

#180903 - $15.00 USD Received 29 Nov 2012; revised 11 Jan 2013; accepted 11 Jan 2013; published 6 Mar 2013

The significance of G_T, G_A is that the parabolic width of the transverse or axial intensity point spread function is then $1/(G_T)^{1/2}, 1/(G_A)^{1/2}$, respectively, compared with the values for the unobstructed pupil. The maximum value of G_T for a positive pupil is 3, corresponding to cosine fringes, as formed by two interfering plane waves. This can regarded as the 2D analog of a Bessel beam, as generated by a thin annulus, in the 3D case. As for the 3D case, we also have for the fractional power transmission of the pupil

$$E = \frac{1}{2}\int_{-1}^{1} |P(\xi)|^2 d\xi / \left(P_{\max}\right)^2, \tag{10}$$

so that the intensity at the focus normalized by the focused power is $F = S/E$. S, G_T, G_A, E and F are all unity for an unobstructed pupil. These parameters can be used to investigate the focal performance of various designs of mask, without the necessity to evaluate directly the focal distribution.

3. Pupil filters for maximally flat axial intensity

From Eq. (2) with $P(\xi) = 1$, the amplitude of the focused field for a slit pupil element extending from $\xi = a$ to $\xi = b$ in the scalar, Fresnel regime, can be written in terms of error functions as [15]

$$U(v,u) = -i\sqrt{\frac{\pi N}{2u}}\, e^{ikz} \exp\left[\frac{iv^2(u+2\pi N)}{4\pi N u}\right]\left\{\mathrm{Erf}\left[\frac{(1+i)(bu-v)}{2\sqrt{u}}\right] - \mathrm{Erf}\left[\frac{(1+i)(au-v)}{2\sqrt{u}}\right]\right\}. \tag{11}$$

We now use the same approach that we used to calculate maximally flat filters for the rotationally symmetric case [9]. Along the axis $v = 0$, and restricting our attention to the case of large *N*, we expand the error functions as power series in *u*, put the lowest order terms to zero to give a flat axial intensity, and solve the resulting simultaneous nonlinear equations. For three symmetric elements of alternating sign $(+1, -1)$, we can make the u^2 term zero, so that $G_A = 0$. For five symmetric elements, we can make the terms in u^2 and u^4 zero, and for seven symmetric elements we can also make the term in u^6 zero. The resulting solutions for the boundaries of the pupil elements $\xi = \pm m_i$ are shown in Table 1, together with *S* and G_T calculated from Eq. (8). For three or five elements, there are two different solutions in each case. For seven elements there are four solutions. In Table 1 we list these in decreasing G_T (increasing *S*) for each order. We also introduce the parameter *W*, the normalized axial length to the 90% point in intensity, which is calculated from the axial intensity.

Table 1. Values of Various Parameters for Filters with 1, 3 5 or 7 Elements

Filter	m_1	m_2	m_3	W	S	G_T	$S/(G_T)^{1/2}$	WG_T
1				1	1	1	1	1
3a	0.23630			2.58	0.278	1.846	0.21	4.76
3b	0.89076			2.59	0.611	0.529	0.84	1.37
5a	0.15957	0.47648		4.25	0.134	2.162	0.09	9.19
5b	0.78061	0.94754		4.25	0.444	0.375	0.73	1.59
7a	0.12166	0.36267	0.59966	5.99	0.080	2.337	0.05	14.00
7b	0.15191	0.42355	0.93925	5.62	0.112	1.528	0.09	8.59
7c	0.18658	0.84615	0.95331	5.65	0.170	1.129	0.16	6.38
7d	0.70018	0.87347	0.96899	5.90	0.350	0.293	0.65	1.73

#180903 - $15.00 USD Received 29 Nov 2012; revised 11 Jan 2013; accepted 11 Jan 2013; published 6 Mar 2013

The overall S versus G_T performance is illustrated in Fig. 1. The behavior for general symmetrical 3 element binary phase filters is also shown: there are two branches, for $G_T \geq 1$ and $G_T \leq 1$.

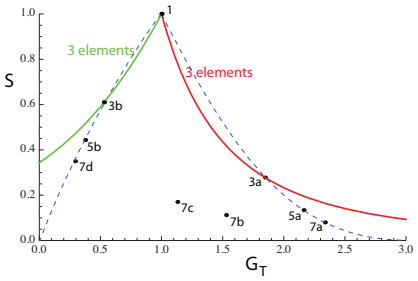

Fig. 1. The variation of the Strehl ratio S with transverse gain G_T for different filters. The maximally flat filters 3a, 5a, 7a lie on the dashed line indicated. The maximally flat filters 3b, 5b, 7d lie on another dashed line. The behavior for general symmetrical 3 element binary phase filters is also shown as solid lines: there are two branches, shown in red for $G_T \geq 1$ and in green $G_T \leq 1$.

The first solutions listed in Table 1 for each number of elements (Nos. 3a, 5a, 7a) approximate to a cosine beam, with strong side lobes, becoming closer to a cosine beam as the number of elements increases ($G_T \to 3$). The axial and transverse intensity variations calculated from Eq. (2) are shown in Fig. 2(a) and 2(b), where they are plotted against the optical coordinates given by Eqs. (3), 4. The last solutions listed in Table 1 for each number of elements (Nos. 3b, 5b, 7d) exhibit $G_T \leq 1$ and weak side lobes, with the axial and transverse intensities shown in Fig. 2(e) and 2(f). As the number of elements increases, this solution tends to a plane wave ($G_T \to 0$). The other solutions for seven elements (Nos. 7b, 7c) are shown in Fig. 2(c) and 2(d): they also have strong side lobes. The side lobe behavior is indicated by the parameter $S/(G_T)^{1/2}$ in Table 1, which is a measure of the fraction of the power in the central lobe. It is seen that the last solutions for each number of elements exhibit much larger values for this parameter, indicating that the side lobes are weak.

Because the length of the focus is proportional to $W \sin^{-2}\alpha$ and the width of the beam is inversely proportional to $\sqrt{G_T}\sin\alpha$, an overall performance parameter WG_T is independent of $\sin\alpha$. This increases with the number of elements, as shown in Table 1. For solution 7d, the transverse width is about twice that for an unobstructed slit aperture, but the focal depth is increased nearly six times, and the Strehl ratio is also quite high at 0.35. Hence to maintain a particular depth of focus, a higher numerical aperture can be used for a greater number of elements, thus giving a smaller transverse width.

#180903 - $15.00 USD Received 29 Nov 2012; revised 11 Jan 2013; accepted 11 Jan 2013; published 6 Mar 2013

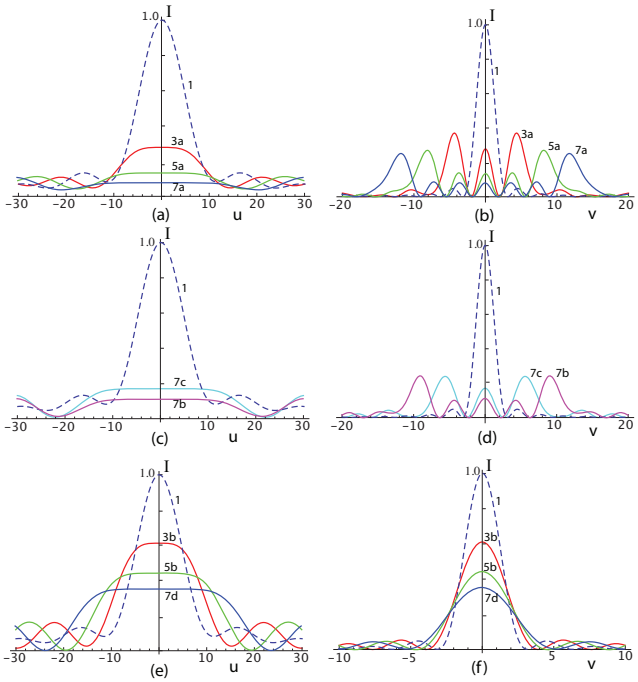

Fig. 2. The axial (a, c, e) and transverse (b, d, f) intensity variations of the different maximally flat filters. (a, b) show filters 3a, 5a, 7a. (c, d) show filters 7b, 7c. (e, f) show filters 3b, 5b, 7d. The curves for an unobstructed slit pupil are shown as dotted lines.

4. Spherical focusing with extended focal depth

In our previous papers we investigated the properties MF filters for spherical lenses [9, 10]. We concentrated on the solutions that give the narrowest central lobe, which approximate to Bessel beams but exhibit strong side lobes. For either two or three elements there were two different solutions, while for four or five elements there were four solutions. In the light of our study for cylindrical lenses, we now consider the broad solutions for the spherical case, which exhibit weak side lobes. Actually some results for these cases were given in the previous papers: the values for S are the same as for the narrow solutions, while the sum of G_T for the broad and narrow solutions is equal to 2 [9]. Meridional plots were also presented [10]. In Table 2 we present designs (rings of normalized radius ρ_i of alternating sign), together with values of the performance parameters, for the solution with weak transverse side lobes. The transverse normalized intensity variation is shown in Fig. 3. As the number of elements increases, the curves become broader, but the side lobes are not much stronger than for an unobstructed circular pupil. The overall performance parameter WG_T increases with number of elements, indicating that a useful combination of depth of field and beam width can be achieved.

Table 2. Values of Various Parameters for Circular Filters with 1-5 Elements

Filter	ρ_1	ρ_2	ρ_3	ρ_4	W	S	G_T	SG_T	WG_T
1					1	1	1	1	1
2	0.3992				2.62	0.464	0.607	0.76	1.76
3	0.8247	0.9581			4.29	0.275	0.458	0.60	1.96
4	0.7534	0.8958	0.9744		6.01	0.184	0.372	0.50	2.24
5	0.6980	0.8390	0.9301	0.9827	7.77	0.133	0.316	0.42	2.46

#180903 - $15.00 USD Received 29 Nov 2012; revised 11 Jan 2013; accepted 11 Jan 2013; published 6 Mar 2013

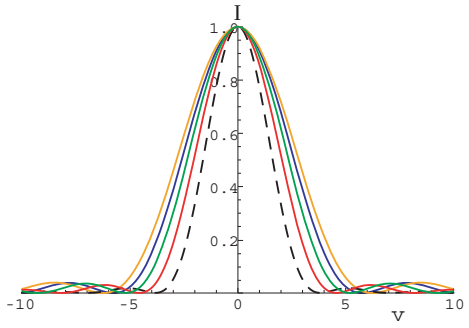

Fig. 3. The transverse variation in normalized intensity if the focal plane of a spherical lens with MF filters of 1-5 elements, for the broad solution. 1 element (black dashed line) corresponds to an unobstructed circular pupil. The curves get wider as the number of elements increases. Red: 2 elements. Green: 3 elements. Blue: 4 elements. Orange: 5 elements.

5. Discussion

We have shown numerically how binary phase filters to increase the focal depth of a cylindrically focusing system can be generated using an analytic method. The resulting designs giving a narrow transverse peak exhibit very strong side lobes. While these may be useful for generating arrays of flat-topped fringes, they are unsuitable for applications where a single light sheet, or a line in 2D, is desired. On the other hand, designs with a broad transverse peak have weak side lobes and a uniform axial intensity. The combination of transverse width and depth of field can give a superior performance to that of an unobstructed slit aperture. These designs are suitable for generating light sheets, or for producing a line focus in two-dimensional systems such as planar waveguides and plasmonics.

In our previous studies [10], we showed how filters for spherical focusing are robust to small variations in dimensions, such that a practical liquid crystal modulator could be satisfactorily employed. Simulations show that the cylindrical filters are also quite robust.

The fact that it is possible to produce a flat axial behavior, over an extended range, with transverse behavior very different from a cosine beam is in itself intriguing.

#180903 - $15.00 USD Received 29 Nov 2012; revised 11 Jan 2013; accepted 11 Jan 2013; published 6 Mar 2013